Kinetics and Catalysis, Vol. 46, No. 2, 2005, pp. 282–294. Translated from Kinetika i Kataliz, Vol. 46, No. 2, 2005, pp. 302–315.

Development of Contactless Methods for Directly Measuring the Temperature of Nanoparticles of the Active Component in Operating Supported Catalysts

L. M. Plyasova[1], V. V. Aver'yanov[2], E. A. Paukshtis[1], T. A. Kriger[1], A. A. Khasin[1], and V. N. Parmon[1,2]

[1] *Boreskov Institute of Catalysis, Siberian Division, Russian Academy of Sciences, Novosibirsk, 630090 Russia*

[2] *Novosibirsk State University, Novosibirsk, 630090 Russia*

Received April 1, 2004

Abstract—*In situ* X-ray diffraction and spectroscopic methods for direct contactless measurement of the temperature of nanoparticles of the active component in operating supported catalysts are considered. These methods have provided convincing evidence that the temperature of nanoparticles of the active component may differ significantly from the support temperature during a very exothermic reaction.

The temperature of the active component of a catalyst is the most important parameter of any catalytic process. It is usually supposed that the temperature of the active component of a heterogeneous catalyst is equal to the catalyst grain temperature measured by standard methods, e.g., with a thermocouple placed near or inserted into a catalyst grain. However, in exothermic catalytic reactions, heat is released primarily on the active component of the catalyst. Therefore, for supported metal catalysts, which are characterized by a significant difference in thermal conductivity between the active component and the inert support, there can be a considerable overheating not only of the entire catalyst grain relative to the environment, but also of the active component particles relative to the support and other catalytically inactive components of the grain.

The possibility of overall overheating of catalyst grains and the effect exerted on this overheating by the gas flow temperature and other reaction conditions have been the subject of numerous studies. For example, Slin'ko *et al.* [1, 2] studied, in detail, the temperature conditions under which catalyst grains operate in hydrocarbon hydrogenation on Pt/Al_2O_3. Catalyst grain temperature was directly measured with a thermocouple. However, this method provides only the average temperature of the grain in contact with the thermocouple. When the catalyst is fine metal particles on a support surface, standard contact methods cannot measure the temperature of these particles independently of the support.

Kellow and Wolf [3] performed direct *in situ* IR thermography of the surface of a Pd/SiO_2 catalyst and demonstrated the nonuniformity of the spatial temperature distribution on the surface of this catalyst in CO oxidation. However, the low spatial resolution and specific features of optical thermography prevented them from correlating the temperature measured with the phase composition of components of the catalyst and, accordingly, from making inferences as to the temperatures of individual surface phases in the operating catalyst.

Nonetheless, quantitative estimates of the expected overheating of particles of the active component in a operating catalyst showed [4] that the overheating of active metal particles relative to the inert support in highly exothermic catalytic reactions can be tens and even hundreds of degrees. Therefore, this overheating can significantly affect the observed properties of the entire catalyst. For example, for supported metal catalysts for deep hydrocarbon oxidation (e.g., $Pt/\gamma\text{-}Al_2O_3$ with a Pt particle size of about 10 nm), calculations predicted that the overheating of particles of the active component of the catalyst relative to the inert support can be up to 200 K at a support temperature of ~900 K. It was experimentally shown [5, 6] that CO oxidation on a number of Cu-, Pt-, Pd-, and Ni-containing supported catalysts is characterized by an ignition–extinction temperature hysteresis. The amplitude of this hysteresis ranges from 20 to 100 K and is assumed to be also related to the overheating of active component particles.

Obviously, knowledge of the true temperature of the active component in an operating catalyst is fundamentally important to understanding the behavior of any catalytic reaction. In particular, this is necessary to calculate the activation energy or the expected process rate.

There has been little progress in the field of direct contactless measurement of particle temperature for fine-particle active components in operating catalysts. Nevertheless, there are X-ray diffraction and IR-spectroscopic methods suitable for contactless temperature

0023-1584/05/4602-0282 © 2005 MAIK "Nauka/Interperiodica"

measurement. X-ray diffraction methods either study the temperature dependence of unit cell parameters for a chosen phase of the active component of a supported catalyst or measure the amplitude of thermal vibrations of atoms of the metal phase in the catalyst during the reaction. IR spectroscopy is based on the fact that all heated bodies emit IR radiation whose parameters depend on temperature.

The purpose of the present work was to develop and experimentally test high-temperature X-ray diffraction and IR emission spectroscopy methods for directly measuring the true temperature of nanoparticles of the active component in supported catalysts.

EXPERIMENTAL

The X-ray diffraction method was tuned using a 15% Ni/SiO_2 catalyst, which is active in the exothermic reaction of CO hydrogenation [7]. The catalyst was prepared by precipitation from an aqueous solution of nickel nitrate with subsequent thermolysis of the precipitate to nickel oxide in flowing argon at 500°C and activation in flowing hydrogen at ~500°C. The active component of the catalyst was nanocrystalline particles of nickel metal with a mean size of (20 ± 2) nm, which were distributed over the surface of amorphous silica gel with a specific surface area of ~100 m^2/g.

IR emission spectroscopy was carried out on the following catalysts: an Ni/SiO_2 catalyst similar to the catalyst used in the X-ray diffraction study, Ni/MgO containing 50% Ni, Co/Al_2O_3 containing 20% Co, and a Pt/glass cloth catalyst that contained 0.1 wt % Pt and was obtained by impregnating preleached glass fibers with an $Na_2[Pt(NH_3)_4]$ solution at room temperature [8]. A catalyst powder was compacted into pellets, and then a catalyst pellet or a glass cloth disk was secured in a cell.

X-ray Diffraction Study

The x-ray diffraction study was performed with a Siemens D-500 X-ray diffractometer (Germany) using Cu(Mo)K_α radiation and a graphite monochromator for the diffracted beam. High-temperature experiments were carried out in an X-ray reactor chamber [9], which was mounted on the diffractometer and allowed one to make measurements at temperatures up to 500°C in flowing gas mixtures at controlled heating and gas flow rates. Samples placed in the reactor chamber were preheated in flowing hydrogen to 450°C to remove the oxide film from the surface of metal particles and then cooled to 200°C. Next, a reaction mixture containing 50 vol % CO and 50 vol % H_2 was admitted to the sample being heated in flowing hydrogen. The mean sample temperature was recorded with a Pt/PtRh thermocouple welded to the bottom of the metallic sample holder. Special experiments showed that, for a 0.3-mm-thick sample pressed into a stainless steel cell, the temperature difference between the diffracting surface of the sample and the bottom of the sample holder was no larger than 5 K.

X-ray diffraction patterns were recorded at 2θ = 25°–105° by pointwise scans in 0.02° steps. Unit cell parameters were determined from five reflections in the scan range and were refined by least squares according to a published procedure [10]. The accuracy of the determination of the nickel unit cell parameter for the sample studied was $\delta a = \pm 0.0002$–0.0005 Å. Integral reflection intensity was estimated with a relative accuracy of ±5%. While the sample was heated in flowing hydrogen or reaction mixture at a heating rate of 5 K/min, its temperature was measured with a thermocouple and X-ray diffraction was recorded at 25-K intervals in the temperature range 200–450°C.

IR-Spectroscopic Study

For experiments using IR emission spectroscopy, a special cell was made, which served as a plug-flow catalytic reactor (Fig. 1). An internal KBr window was necessary to prevent gas cooling on the external KBr window. Two resistance heaters were used, one of which was mounted directly on the cell and the other served for preheating the incoming gas. The temperatures of the incoming reaction mixture and of the sample, measured with thermocouples, were maintained constant.

A flowing reaction mixture preheated to the sample temperature was admitted to the sample. If CO hydrogenation was studied, the reaction mixture consisted of 33 vol % CO and hydrogen, and if CO oxidation was investigated, the reaction mixture consisted of 2 vol % CO and air. The flow rate of the reaction mixture was 6 or 10 l/h. To measure CO conversion, the gas leaving the cell was passed through a gas analyzer cell. The products were analyzed by IR absorption spectroscopy on a Shimadzu FTIR 8300 Fourier-transform IR spectrophotometer (Japan); all spectra were recorded by making 50 scans at a resolution of 4 cm^{-1}.

The cell was put into the place of the radiation source of a Spectrolab Interspec 2020 IR spectrophotometer, and the emission spectra of the sample were recorded at different thermocouple-measured sample temperatures. The reference spectra were the emission spectra of the sample at the same thermocouple-measured temperatures in an inert atmosphere. The emission spectra of the catalyst were recorded by performing ten scans (at an acquisition time of 80 s) at a resolution of 4 cm^{-1}.

The spectra were recorded at thermocouple-measured temperatures of 150–400°C at intervals of 20 or 50 K.

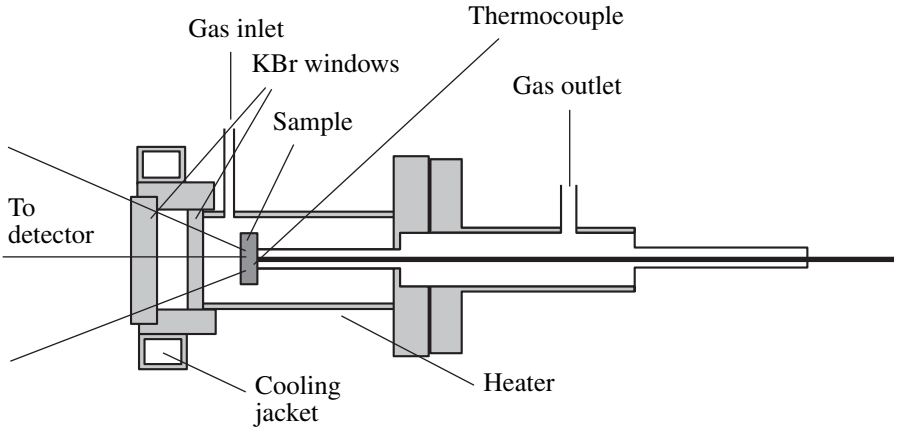

Fig. 1. IR-spectroscopic temperature measurement cell.

RESULTS AND DISCUSSION

Separate Measurement of the True Temperature of a Chosen Phase by in situ X-ray Diffraction

Temperature determination from the temperature dependence of unit cell parameters. Heating of a substance is accompanied by its thermal expansion and, as a consequence, a change in the unit cell parameters and size. Analysis of this change is widely used to determine the thermal expansion coefficients of substances [11].

In temperature determination from the temperature dependence of unit cell parameters, it is necessary to find the positions of diffraction peaks in an X-ray diffraction pattern and then calculate the interplanar spacings d_{hkl}, which are related to unit cell parameters by quadratic expressions. For example, for cubic symmetry, $1/d_{hkl}^2 = (h^2 + k^2 + l^2)/a^2$, where a is the unit cell parameter and h, k, and l are Miller indices [12]. The temperature dependence of the parameter a for many substances, including catalytically active metals, is reported in some handbooks (see, e.g., [13]). Thus, a comparison of the function $a(T)$ determined *in situ* during a reaction with the function $a(T)$ found in an inert medium or with reference $a(T)$ data allows one to determine the change in a during the reaction and, accordingly, the true temperature of the active component in the operating catalyst.

Figure 2 presents until cell parameter data for metallic Ni in the catalyst Ni/SiO_2 as a function of the average catalyst temperature between 200 and 450°C in a nonreactive medium of pure hydrogen (curve *1*) and in a reactive mixture of CO and H_2 (curve *2*). Figure 2 shows that, upon heating in the hydrogen medium to 450°C, the lattice parameter a of metallic Ni increases linearly with temperature. At a thermocouple-measured grain temperature of 200°C, the unit cell parameter a of Ni in the reaction mixture of CO and H_2 almost coincides with that in hydrogen at the same temperature. However, as the mean catalyst temperature increases to 450°C, there is a gradually increasing excess of the Ni unit cell parameter a over its value in hydrogen. This excess is significantly larger than the measurement error. Under our experimental conditions, the error δa of determination of a was $(2–5) \times 10^{-4}$ Å, which is several times smaller than the total observed excess of the parameter a ($(12–27) \times 10^{-4}$ Å). It is reasonable to assume that the excess of the Ni unit cell parameter a in the $CO + H_2$ medium over its value in pure hydrogen is a consequence of the overheating of the active component because of the heat release in the exothermic CO hydrogenation reaction

$$\mathrm{CO} + 3\mathrm{H_2} \longrightarrow \mathrm{CH_4} + \mathrm{H_2O} - 210\ \text{kJ/mol}\ (\Delta_r H^0_{298}). \quad \text{(I)}$$

Below, one can find the excess Δa of the unit cell parameter a of metallic nickel in the Ni/SiO_2 catalyst upon heating in the $CO–H_2$ medium over its value upon heating in pure hydrogen and the corresponding overheating ΔT relative to the thermocouple-measured catalyst grain temperature T.

T, °C	250	300	350	400
Δa, Å	0.0009	0.0013	0.0022	0.0029
ΔT, °C	28	44	58	77

Note that the accuracy of determination of the unit cell parameter a, $\delta a = (2–5) \times 10^{-4}$ Å, corresponds to the accuracy of determination of catalyst overheating, δT = 8–10 K.

The temperatures of the active component (metallic nickel) directly measured in the $CO + H_2$ medium are indicative of its overheating, which gradually increases with an increase in the catalyst grain temperature and reaches ~80°C at a catalyst grain temperature of 400°C.

Previously [14], using a similar method, we separately measured the temperatures of the active component and the support for Ni/MgO catalyst in reaction (I). Since

both components of this catalyst were in the crystalline state, it was possible to separately measure the true temperature of not only the active component but also the support. However, the accuracy of determination of the unit cell parameters and temperature for the Ni/MgO catalyst turned out to be much lower than that for the above Ni/SiO_2 catalyst. This was because of smaller nickel particle size (6–8 nm) and lower nickel content (<10 at. %) of the Ni/MgO catalyst, which led to lower accuracy of determination of both the unit cell parameter ($\delta a = 30 \times 10^{-4}$ Å) and temperature ($\delta T = 25$°C).

Obviously, to use the method proposed for direct separate measurement of the temperatures of the active component and the support, it is necessary that both components be crystalline. Unfortunately, the supports in most catalysts are amorphous to X-rays. In this case, one can measure only the temperature of the active component, which is crystalline. The sensitivity and accuracy of the method proposed for direct contactless temperature measurement depend on the accuracy of measurement of unit cell parameters. In turn, this is determined by the concentration of the active component, the size of its particles, the diffraction power of its atoms, and lattice symmetry. For catalysts with developed surface, small particle sizes of the active component, and low concentrations of the finely dispersed active component, accurate measurement of the parameter a may be impossible. Therefore, the most suitable objects to be studied by the method proposed are supported metal catalysts containing metals with high diffraction power, e.g., platinum group metals crystallizing in highly symmetric structures with the closest packing of atoms (it is desirable that the metal concentration exceed 10 at. %).

Temperature determination from the temperature dependence of the amplitude of thermal vibrations of atoms under real conditions. Another X-ray diffraction method for direct temperature measurement is based on studying the temperature dependence of the amplitude of thermal vibrations of atoms in the crystal lattice.

X-ray diffraction theory says that the thermal vibrations of atoms in crystals decrease the intensity of diffraction peaks according to the law $\exp(-2B\sin^2\theta/\lambda^2)$, where $B = 8/3\pi^2\langle u^2\rangle$, θ is the reflection angle, λ is the radiation wavelength, and $\sqrt{\langle u^2\rangle}$ is the amplitude of thermal vibrations of atoms (the root-mean-square displacement of atoms from equilibrium because of thermal vibrations, a function of temperature) [15]. The temperature of a scattering object can be found by comparing the measured root-mean-square displacements with the displacement predicted by the Debye formula [16]

$$\langle u^2\rangle = 9h^2T/4\pi^2mk\Theta^2[\Phi(x) + x/4], \qquad (1)$$

where $x = \Theta/T$; Θ is the characteristic temperature of the crystal, which is determined by the interatomic forces in the crystal [16]; T is the absolute temperature of the scattering object; h is Planck's constant; m is the weight of a scattering atom; k is the Boltzmann constant; and $\Phi(x)$ is the Debye function (see [16]).

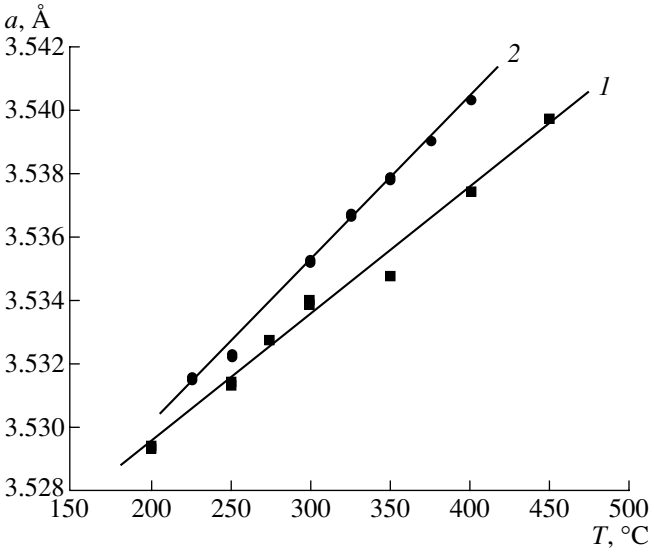

Fig. 2. Unit cell parameter a of metallic nickel nanoparticles in the catalyst Ni/SiO_2 in (*1*) a nonreactive medium of pure hydrogen and (*2*) a reactive mixture of $CO + H_2$ vs. average thermocouple-measured temperature upon heating of the sample.

The characteristic temperature Θ of crystals is well known for many pure and well-crystallized metals (see, e.g., [16, 17]).

Curve *1* in Fig. 3 presents the $\sqrt{\langle u^2\rangle}$ versus T plot calculated for large-crystal Ni^0, for which $\Theta = 375$ K [17].

To determine the amplitude $\sqrt{\langle u^2\rangle}$ of root-mean-square displacements or the characteristic temperature Θ, one can use a published procedure [18] based on measuring the integral intensity of diffraction lines over a wide angle range. The integral intensity I of a diffraction line is expressed as

$$I(hkl) = I_0CHLPGF^2_{hkl}\exp(-2B\sin^2\theta/\lambda^2), \qquad (2)$$

where I_0 is the intensity of the primary X-ray beam, LPG is the angular factor, H is the multiplicity factor, C is the absorption factor, F^2_{hkl} is the structure factor, and $\exp(-2B\sin^2\theta/\lambda^2)$ is the temperature factor [12, 18].

If the structure of the object is known, all terms in expression (2), except I_0 and $\exp(-2B\sin^2\theta/\lambda^2)$, can be calculated.

Denoting $K = CHLPGF^2_{hkl}$, we obtain

$$I(hkl)/K = I_0\exp(-2B\sin^2\theta/\lambda^2), \qquad (3)$$

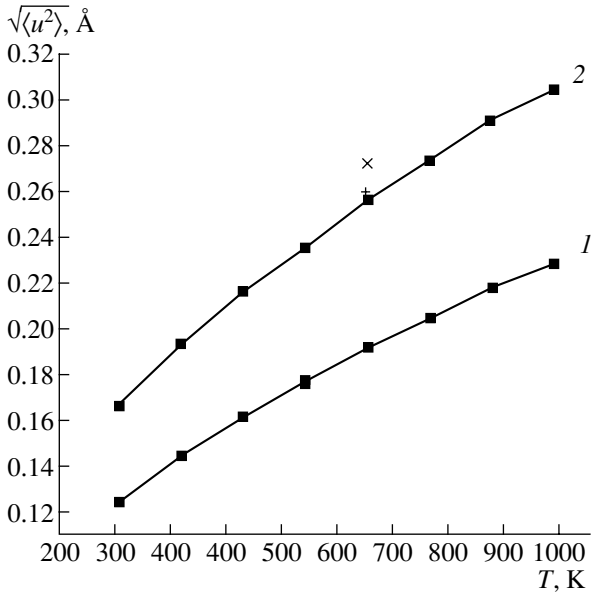

Fig. 3. Calculated amplitude $\sqrt{\langle u^2 \rangle}$ of thermal vibrations of nickel atoms at Θ = (*1*) 375 and (*2*) 280 K vs. *T*. The plus (+) and cross (×) signs denote the experimental $\sqrt{\langle u^2 \rangle}$ value at a thermocouple-measured temperature of 400°C in an unreactive medium of pure hydrogen and a reactive mixture of CO and H_2, respectively.

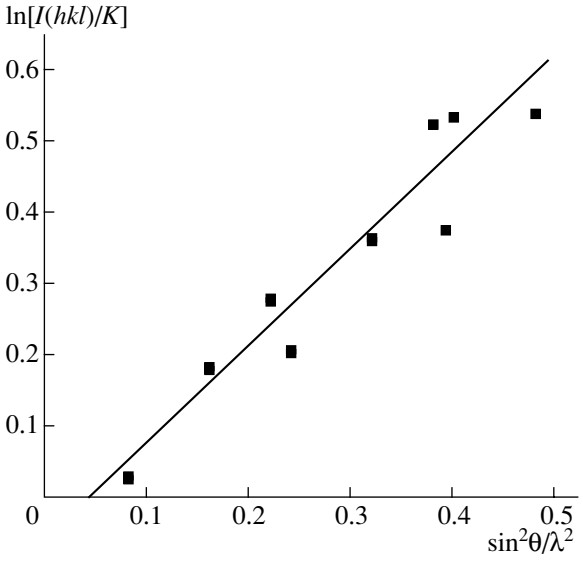

Fig. 4. Experimental ln*I*(*hkl*)/*K* vs. $\sin^2\theta/\lambda^2$ data for nickel metal nanoparticles in the catalyst Ni/SiO_2 in air at room temperature (MoK_α radiation).

whence $\ln\{I(hkl)/K\} = \ln I_0 - 2B\sin^2\theta/\lambda^2$.

Thus, the experimental function *I*(*hkl*) should be linearized in the anamorphoses $\ln\{I(hkl)/K\} \longleftrightarrow \{\sin^2\theta/\lambda^2\}$. From the slope of the straight line, one can find *B* and, hence, $\sqrt{\langle u^2 \rangle}$ and then calculate Θ from Eq. (1).

As an example, Fig. 4 presents the *I* versus $\sin^2\theta/\lambda^2$ plot linearized on these coordinates, which was used to determine the parameter Θ for a hydrogen-prereduced Ni/SiO_2 sample with a coherently scattering region of ~20 nm for Ni in air at room temperature. The Θ value determined from Fig. 4 for this sample is 280 ± 5 K, which differs significantly from the reference data [17] according to which Θ for bulk nickel is 375 K.

The observed discrepancy in Θ is probably related to the particle size of nickel. Indeed, it is well known that crystallite size has an effect on many physicochemical properties of solids, including interatomic forces [19, 20]. For example, it is reported that Θ for nanosized nickel is 293 ± 7 K [20], while Θ = 375 K for coarse nickel crystals.

For metals in supported catalysts, the metal particle size is small and the coherently scattering domains are much narrower than 100 nm; for the sample studied, the coherently scattering domain is ~20 nm. Therefore, the application of the method proposed is complicated by the necessity of additionally determining the characteristic temperature Θ of a substance under investigation at a particle size of interest. Figure 5 shows how the characteristic temperature Θ depends on the Ni particle size in the range from 5 to 30 nm [21]. It is seen that, in this range, the characteristic temperature indeed depends on the Ni particle size. According to these data, for Ni particles with the coherently scattering domain ~20 nm, Θ is also close to 280 K. This tendency for Θ to decrease with decreasing the particle size is also characteristic of other nanocrystalline materials [19, 20].

After finding Θ, in order to determine the temperature dependence of $\sqrt{\langle u^2 \rangle}$ for nickel particles of this catalyst with a coherently scattering domain of ~20 nm, one can use the measured Θ value in formula (1) (Fig. 3, curve *2*) and, comparing the temperature dependence of $\sqrt{\langle u^2 \rangle}$ in the reactive and inert media, find the true temperature of the phase observed during the reaction.

However, it is obvious that this way of directly measuring the temperature of nanoparticles requires the intensity of diffraction peaks to be very accurately determined over a wide range of angles. Unfortunately, this is not always possible for catalysts with low active-component content and takes much time.

To reliably measure the temperature by the method proposed, it is necessary that the increment $\Delta\sqrt{\langle u^2 \rangle}$ in the amplitude of thermal vibrations exceed the measurement error $\delta\sqrt{\langle u^2 \rangle}$. According to works carried out at a modern level (see, e.g., [20]), it is actually impossible to reduce the relative measurement error $\delta\sqrt{\langle u^2 \rangle}$ below 5% of the determined $\sqrt{\langle u^2 \rangle}$ value. Thus, for

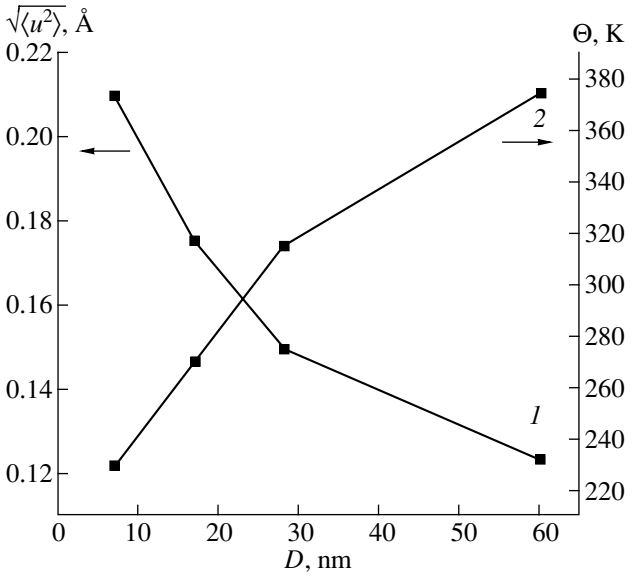

Fig. 5. (*1*) Amplitude $\sqrt{\langle u^2 \rangle}$ of thermal vibrations and (*2*) characteristic temperature Θ vs. coherently scattering region size *D* for metallic nickel nanoparticles (according to [20]).

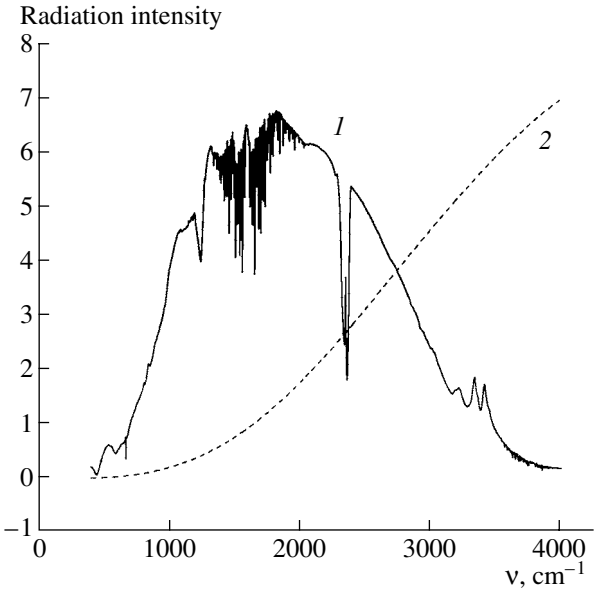

Fig. 6. (*1*) Experimental emission spectrum of the standard radiation source of a IR spectrophotometer with a temperature of 1470 K and (*2*) theoretical curve constructed according to Planck's radiation law for the same temperature.

$\sqrt{\langle u^2 \rangle}$ values of about 0.2–0.25 Å, the error is 0.01–0.015 Å, which in temperature measurement corresponds to an error of 50–75 K. Note that the accuracy of the determination of temperature from the unit cell parameter *a* in our experiments was much better and was 8–10 K. Below, we present the accuracy δT of the measurement of the temperature of the active component in the Ni/SiO_2 catalyst, the accuracy δa of the measurement of the unit cell parameter, and the amplitude $\sqrt{\langle u^2 \rangle}$ of the root-mean-square displacements of atoms in metallic nickel nanoparticles.

δa, Å	$\delta\sqrt{\langle u^2 \rangle}$, Å	δT, °C
$(2–5) \times 10^{-4}$	–	8–10
–	0.01–0.015	50–75

For the Ni/SiO_2 catalyst, we failed to reveal a reliable dependence of the amplitude of thermal vibrations of atoms on the composition of the gas phase and temperature. Only for a sample studied at a thermocouple-measured grain temperature of 400°C in hydrogen and the 1 : 1 H_2–CO mixture did these measurements show that $\sqrt{\langle u^2 \rangle}$ in the hydrogen medium is close to the calculated value (0.26 Å) for the given particle size and $\sqrt{\langle u^2 \rangle}$ in the 1 : 1 H_2–CO mixture is increased to 0.273 Å. The latter value corresponds to an overheating of active component particles of ~80–90 K (Fig. 3). This is consistent with the result obtained from the measured unit cell parameters but is at the limit of the measurement accuracy. One can suppose that the proposed method for direct temperature measurement is more efficient at an overheating of nanoparticles above 100 K throughout the range of average grain temperatures.

Thus, the measurement of the overheating of the active component by measuring the unit cell parameters is more sensitive and more accurate than the measurement based on determining the integral intensities of diffraction lines and, correspondingly, the amplitudes of thermal vibrations.

Note that the overheating of the active component during a reaction can be detected from a change in the intensity of diffraction peaks without preliminarily determining its characteristic temperature. For this purpose, it is sufficient to measure the ratio of the integral intensities of the two lines that are farthest from each other but intense enough in X-ray diffraction patterns recorded at the same catalyst grain temperature in different media (e.g., for the given catalyst, in pure hydrogen and the CO–H_2 medium). The determination of the intensity ratio enables one to eliminate the effect of the geometric recording conditions. Let α_1 and α_2 be the ratios of the intensities of the corresponding lines under given recording conditions:

$$\alpha_1 = I_{hkl}/I_{mnp} \text{ and } \alpha_2 = I'_{hkl}/I'_{mnp}, \quad (4)$$

where I_{hkl} and I_{mnp} are the integral intensities of the diffraction lines (*hkl*) and (*mnp*), respectively, and the primes denote other recording conditions.

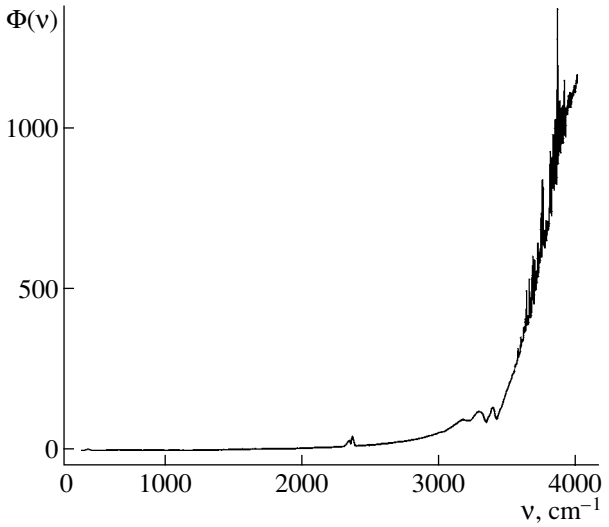

Fig. 7. Calibration function Φ(ν) for the spectrophotometer detector.

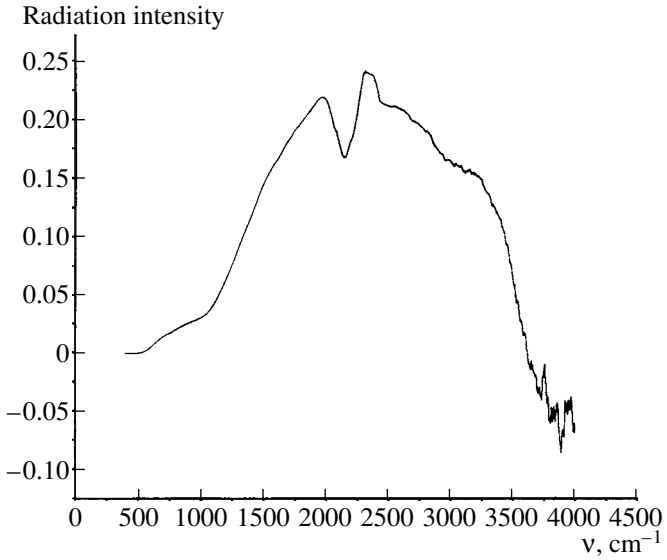

Fig. 8. IR emission spectrum of the Ni/SiO_2 catalyst at 400°C in flowing inert gas (nitrogen).

According to Eq. (3), the ratio α_1/α_2 depends only on the ratio of the thermal factors. Taking the logarithm of the ratio α_1/α_2 yields

$$\ln(\alpha_1/\alpha_2) = 16\pi^2/3\lambda^2(\sin^2\theta_{hkl} - \sin^2\theta_{mnp})\Delta u^2, \quad (5)$$

where θ_{hkl} and θ_{mnp} are the reflection angles for the reflections (*hkl*) and (*mnp*), respectively, and $\Delta u^2 = \langle u_1^2 \rangle - \langle u_2^2 \rangle$ is the change in the squared amplitude of root-mean-square displacements with a change in the environment of a nanoparticle.

An analysis of the experimental value of $\ln(\alpha_1/\alpha_2)$ qualitatively determines whether or not there is overheating without preliminarily calculating the characteristic temperature. And from the plot of $\sqrt{\langle u^2 \rangle}$ versus the average grain temperature (Fig. 3), one can find the overheating ΔT corresponding to the increment in the amplitude of root-mean-square displacements during the exothermic reaction.

In principle, the direct measurement of temperature in catalysts with a low concentration of fine metal particles can also be performed by the radial atomic distribution method by finding the root-mean-square displacements of atoms from the half-widths $\langle \Delta R_k^2 \rangle$ of the peaks in the radial atomic distribution curve [22]

$$\langle \Delta R_k^2 \rangle = 0.18\, L_{1/2}^2, \quad (6)$$

where R_k is the radius of the *k*th coordination sphere and $L_{1/2}$ is the half-width of the peak of the radial atomic density distribution function.

Note, however, the high laboriousness of the radial atomic distribution method, because of which we have not hitherto tested it.

Determination of the Temperature of the Active Component in Operating Catalysts by IR Emission Spectroscopy

The determination of temperature by analyzing the emission spectra of real bodies is a complex problem because of the large difference in spectral characteristics between ideal objects, for which thermal radiation laws are formulated, and real systems, for which emission spectra are recorded and temperature is measured. Nonetheless, in some cases, one can achieve quite an acceptable measurement accuracy.

In the literature, several approaches to measuring temperature using emission spectra have been described. For example, temperature can be calculated if the total emission of an object is known according to the Stefan–Boltzmann law

$$W = \alpha\sigma T^4, \quad (7)$$

where *W* is the power emitted by a unit area of a radiator into a hemisphere, σ is the Stefan–Boltzmann constant, *T* is the absolute temperature of the radiator, and α is the emissivity factor.

Temperature measurement by this method is complicated by the necessity of recording all of the energy emitted, taking into account both lost and additional radiation emitted by the cell, the holder, etc. This method is also rather difficult to use because of the fact that not ideal blackbodies, but real objects, are usually studied. For example, for objects of nanometer size, it is impossible to use published data on the emissivity factors measured for bulk samples.

The measurement of the temperature of an object by studying its absorption spectra can be performed by analyzing the position ν_{max} of the maximum of the thermal radiation line using Wien's displacement law,

$$\nu_{max} = 2.822kT/h, \quad (8)$$

where k is the Boltzmann constant and h is Planck's constant. This temperature measurement method requires one to sufficiently accurately determine the position of the maximum of the thermal radiation line. This is a complex problem that imposes special requirements on emission spectra.

In our opinion, the temperature of a heated body can be most accurately determined using the variational method by approximating the form of the emission spectra of heated bodies by Planck's radiation function,

$$W(\nu, T) = \frac{2\pi h\nu^5}{c^3(\exp(h\nu/kT) - 1)}, \quad (9)$$

where ν is the frequency and c is the speed of light.

In recording thermal emission spectra, first of all, it is necessary to take into account the spectral characteristics of an IR spectrometer, since the response of the detector to the radiation intensity is a function of the radiation frequency. Therefore, a calibration function should initially be constructed. As a standard—a blackbody (graybody)—we chose the standard radiation source of a Spectrolab Interspec 2020 IR spectrometer with a known fixed temperature of 1200°C.

Figure 6 presents the recorded emission spectrum of the standard radiation source of the IR spectrometer and the theoretical curve constructed according to Planck's radiation law for a temperature of 1473 K. The absorption band at 2350 cm^{-1} corresponds to carbon dioxide, and the band at 1250 cm^{-1} corresponds to the absorption by the IR detector.

The calibration function $\Phi(\nu)$ is constructed by dividing the calculated radiation intensity $W(\nu)$ by the measured value $F(\nu)$. To obtain the real emission spectrum from the spectral curve recorded with the instrument, it is necessary to multiply the spectral curve by the calibration function $\Phi(\nu)$. Figure 7 shows the form of the calibration function $\Phi(\nu) = W(\nu)/F(\nu)$ for the spectrometer used. Further calculations were performed under the assumption that the form of the calibration function is independent of the temperature of the emitting sample.

Figure 8 presents the IR emission spectrum of the Ni/SiO_2 catalyst at 400°C in a nitrogen flow. It is seen that the radiation intensity abruptly decreases at frequencies above 3300 cm^{-1}. This is likely to be caused by two factors, one of which is the radiation scattering by the sample, which increases with radiation frequency, and the other is the absorption by OH groups of the support. Because of these factors, the maximum possible temperature that can be determined from the emission of the objects examined is restricted to 550–600°C. Extending the spectral curve to frequencies above 3300 cm^{-1}, one can satisfactorily describe the obtained spectrum by the blackbody radiation function (Fig. 9). The curve is extended under the assumption that the emission spectra of the sample that are recorded at different temperatures have similar forms. However, as Fig. 10 shows, because of the above reasons, the emission spectrum of the sample at 400°C has a steeper slope of the high-frequency branch. It was determined that the spectral curve should be extended for the IR emission spectra of samples at temperatures above 350°C. As is seen from Fig. 10, at lower temperatures, the high-frequency tail of the spectral curve lies within 3300 cm^{-1}.

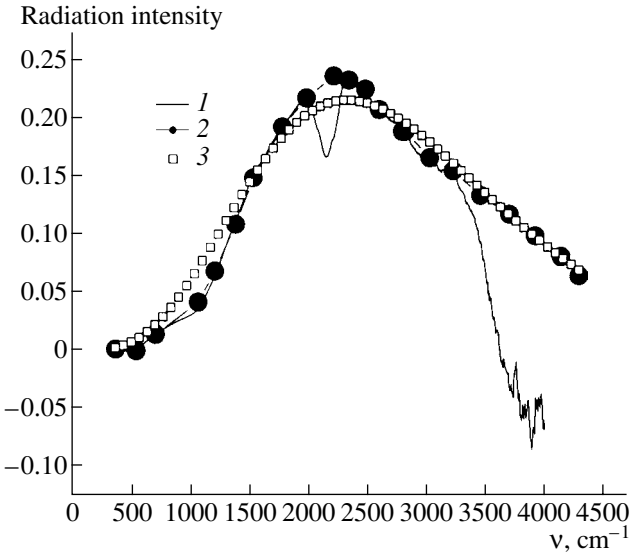

Fig. 9. (*1*) IR emission spectrum of the Ni/SiO_2 catalyst at 400°C, (*2*) extended spectral curve, and (*3*) curve *2* approximated by Planck's radiation function.

The corrected emission spectra $W(\omega, T)$ were approximated with Planck's radiation function by vary-

Table 1. Comparison of the temperatures that are calculated from IR emission spectra and measured with a thermocouple for the catalysts Ni/MgO and $NiSiO_2$ in flowing inert gas (nitrogen)

Thermocouple-measured temperature, °C	Temperature calculated from emission spectra, °C	
	Ni/MgO	Ni/SiO_2
200	200	200
250	240	245
300	295	295
350	345	355
400	390	400

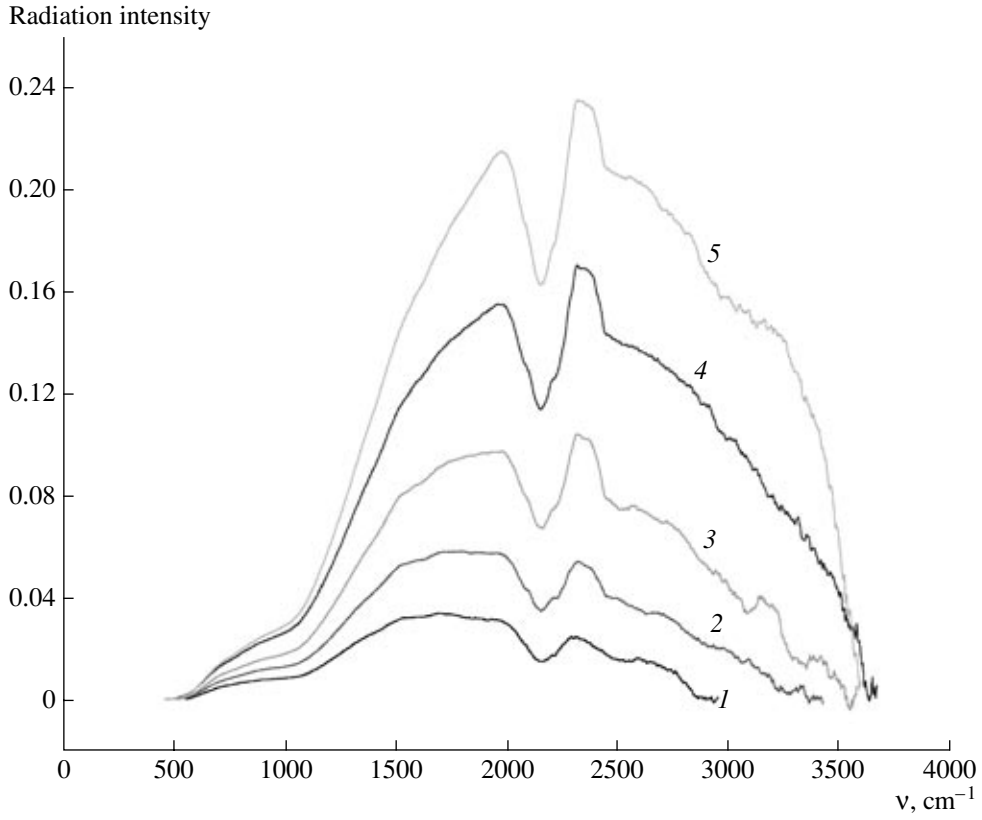

Fig. 10. IR emission spectra of the Ni/SiO_2 catalyst in flowing inert gas (nitrogen) at thermocouple-measured temperatures of (*1*) 200, (*2*) 250, (*3*) 300, (*4*) 350, and (*5*) 400.

ing two parameters and minimizing the variance test χ^2 on the coordinates $W(\omega)$:

$$W(\omega, T) = \frac{P_1\omega^5}{\left(\exp\left(\frac{hc\omega}{kP_2}\right) - 1\right)}. \quad (10)$$

Here, ω is the wavenumber, cm^{-1} and P_1 and P_2 are parameters being varied: P_1 takes into account the emissivity factor under the assumption that this factor is independent of the wavelength, and P_2 is the sought temperature.

As reference spectra for testing the method, we recorded the emission spectra of samples in an inert atmosphere at different average thermocouple-measured sample temperatures. From the emission spectra, the true temperatures of samples were found. Table 1 compares the sample temperatures that were measured with the thermocouple and calculated from the emission spectra. The data presented show that the actual error of temperature determination from the emission spectra does not exceed 10 K, which is quite acceptable for further experiments.

To take into account the emission from the cell walls, the emission spectra of the cell without a sample at different temperatures were recorded. In Fig. 11, each of the curves is the difference of the IR emission spectrum of the Ni/MgO catalyst in an inert gas (nitrogen) flow and the IR emission spectrum of the empty cell, approximated by Planck's radiation function. Thereby, we desired to obtain the emission spectra of the "pure" sample. Below, we present the results of comparing the temperature calculated from these curves with the temperature measured with the thermocouple during recording the spectra.

Thermocouple-measured temperature, °C	200	250	300	350	400
Temperature calculated from spectrum, °C	225	270	320	370	415

The data presented show that the temperature calculated from the difference spectra is 20–25 K higher than the thermocouple-measured temperature. This is most likely to be related, first, to a particular design of the cell, because of which the recorded spectrum of the empty cell exhibits an additional radiation source with a somewhat lower temperature, and, second, to the impossibility of reproducing the exact position of the cell with respect to the detector. Therefore, the subtraction of the IR emission spectra of the empty cell is not

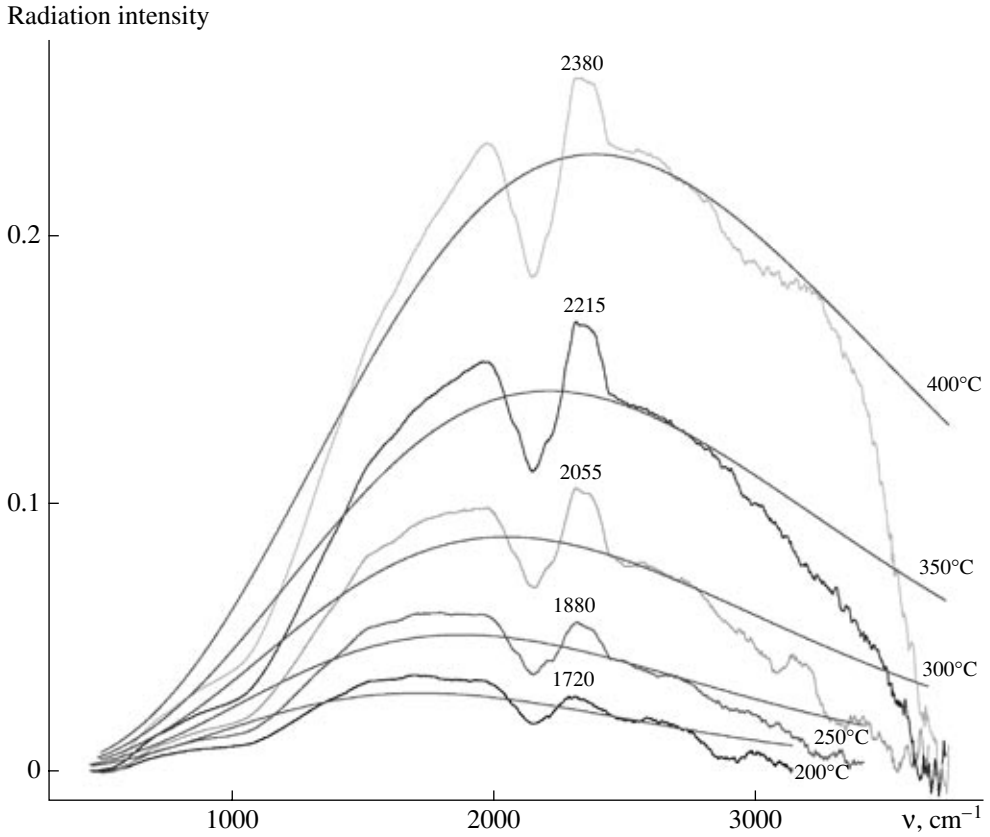

Fig. 11. Difference between the IR emission spectrum of the Ni/MgO catalyst in flowing inert gas (nitrogen) and the IR emission spectrum of the empty cell, approximated by Planck's radiation function, at different temperatures.

quite correct and the spectral curves obtained cannot be assigned to the emission spectra of the pure sample. In further studies, this procedure was not used.

To analyze the emission spectra of the Pt/glass cloth catalyst for obtaining the emission spectra of the pure active component, we initially recorded the emission spectra of glass cloth without platinum in an inert gas (nitrogen) flow. In Fig. 12, each of the curves is the difference of the IR emission spectrum of platinum on glass cloth when there is a reaction or there is no reaction and the IR emission spectrum of glass cloth without platinum at different temperatures. Analysis of the spectral curves demonstrated that the temperature of platinum in an inert gas atmosphere, as well as during the catalytic reaction of CO oxidation by oxygen, is the same and is equal to the thermocouple-measured temperature of the support.

The intensity of the radiation emitted by a heated body is related to its temperature by Stefan–Boltzmann law (7). Based on this law under the assumption that the emissivity factor is the same for both a sample and individual active particles, we calculated the fraction of the overheated surface area. If A_1 and A_2 are the areas under the emission spectra of the sample and overheated particles, respectively, then the fraction α of the overheated surface area is found from the expression $\alpha = \frac{A_2 T_1^4}{A_1 T_2^4}$, where T_1 is the thermocouple-measured temperature of the sample and T_2 is the temperature of active component particles that is determined from Wien's displacement law.

For the curves in Fig. 12, the fraction α of the overheated surface area was estimated. The value obtained turned out to be close to 30% of the total catalyst surface area, although the actual platinum content of the sample was 0.1 wt %. Most probably, the difference between the emission spectra of pure glass cloth and the emission spectra of glass cloth to which platinum was applied are related to the impossibility of exactly reproducing the geometry of the test sample and the reference sample in the cell. Thus, these spectra cannot be assigned to the radiation emitted by the active component. Hence, it follows that only the spectra recorded at fixed positions of the cell and the sample can be correctly compared. This somewhat limits the potential of the method, since, when a sample is reloaded, the cell should be removed. Therefore, the intensities can be compared only for the IR spectra of a once mounted sample.

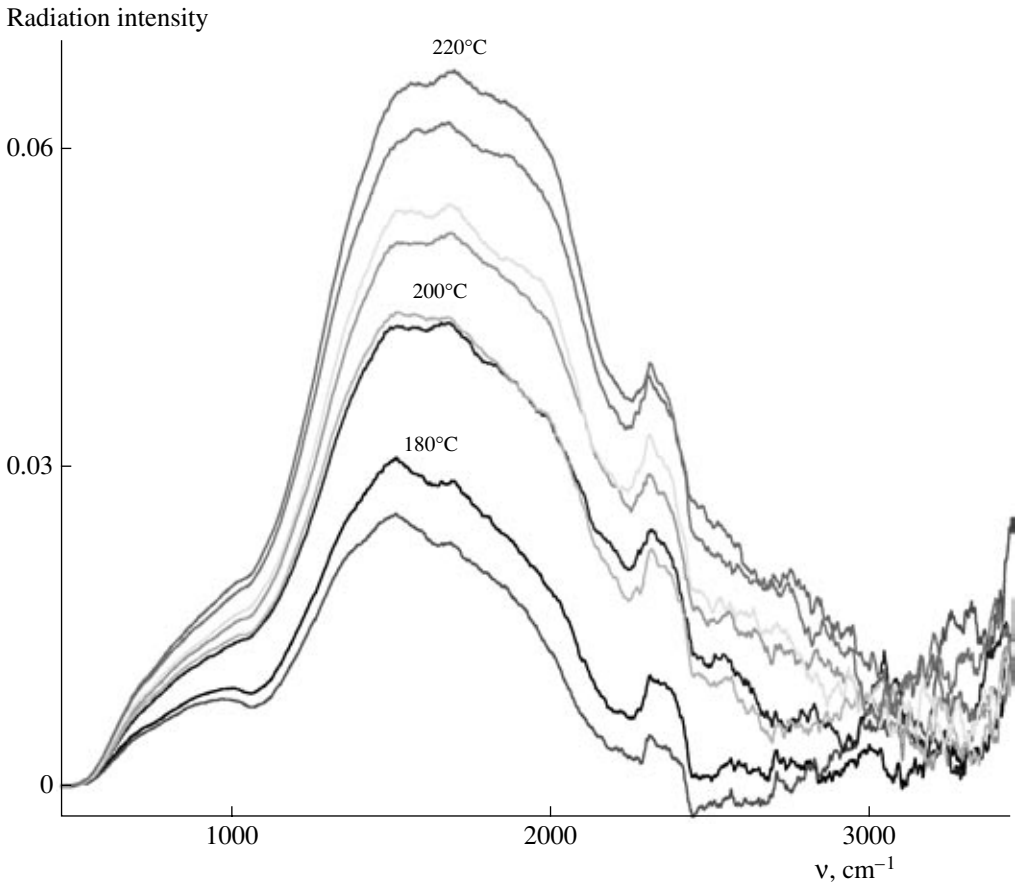

Fig. 12. Difference between the IR emission spectrum of the Pt/glass cloth catalyst and the IR emission spectrum of glass cloth without platinum at different temperatures.

In Fig. 13, each of the curves is the difference of the IR emission spectrum of the operating Pt/glass cloth catalyst during CO oxidation by oxygen and the IR emission spectrum of the same catalyst in an inert gas (nitrogen) flow at different temperatures and flow rates of the reaction mixture, with the spectra being approximated by Planck's radiation function. The positions of the maxima on these curves correspond to the radiation of the overheated surface area. Table 2 summarizes the results of analyzing the emission spectra of the glass

Table 2. Characteristics of the catalytic reaction of CO oxidation by atmospheric oxygen on the catalyst Pt/glass cloth

Thermocouple-measured sample temperature, °C	180	200	200	220	220
CO conversion, %	57	74	35	71	77
Reaction mixture flow rate, l/h	6	6	10	6	10
Position of maximum of emission spectrum of platinum particles, cm^{-1}	1800	1920	1980	1890	1960
Platinum temperature, °C	250	280	300	270	295
Heat release, W per gram catalyst	4.87	5.27	4.98	5.48	10.1
Heat release, W per gram Pt	4.43	4.79	4.53	4.98	9.20
Relative fraction of overheated surface area, %	6	5	5	4.4	5.2

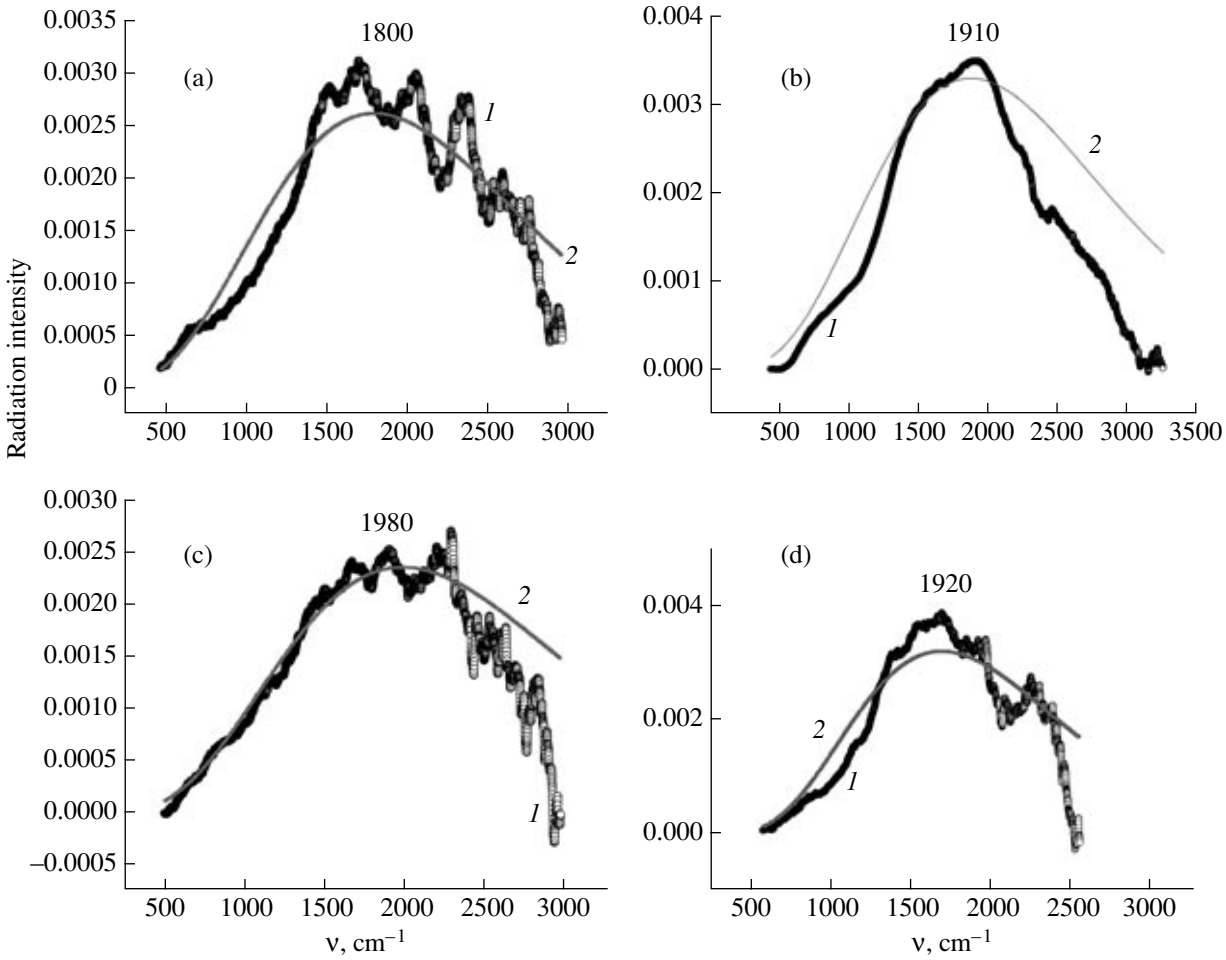

Fig. 13. (*1*) Typical IR emission spectra of the overheated part of the surface of the Pt/glass cloth catalyst and (*2*) curves *1* approximated by Planck's radiation function at different temperatures and flow rates of the reaction mixture: (a) 180; (b) 220; (c) 200°C, 10 l/h; and (d) 200°C.

cloth catalyst. Table 2 shows that the temperature of platinum in the operating catalysts exceeds the support temperature by 50–100 K. In the experiment, the heat release on the active component of the catalyst was calculated to be up to 9–10 kW per gram Pt.

It is significant that platinum nanoparticles are not ideal blackbodies and their emissivity factor depends on the wavelength [23]. Moreover, the maximum of the radiation intensity can be shifted toward either smaller or larger wavenumbers. Therefore, the calculated temperature of platinum particles may differ somewhat from their true temperature. Later, we intend to study the emission spectra of dispersed platinum at different temperatures for using them as reference spectra in determining the temperature of fine platinum particles.

CONCLUSIONS

Several methods for directly measuring the temperature of the active component in operating supported metal catalysts were experimentally tested. For example, by *in situ* X-ray diffraction, we tested the method based on studying the temperature dependence of the unit cell parameters for a chosen individual phase (e.g., the active component of a supported catalyst) and the method based on measuring the amplitude of thermal vibrations of atoms of the active phase in a catalyst during a reaction.

Both methods are applicable to the crystalline states of the active component of a catalyst. The accuracy of the determination of overheating depends on the concentration and particle size of the active component. Other things being equal, the determination of overheating by measuring the unit cell parameters is much more sensitive and much more accurate than the measurement based on recording the amplitudes of thermal vibrations. The measurement of the unit cell parameters enables one to determine the temperature of nanoparticles of the active component of operating catalysts with an accuracy of 5–10 K. The relative temperature measurements in this case turned out to be much more accurate and sufficient for solving many problems involving

the determination of the temperature of the active component.

We also developed a method for the direct contactless measurement of the temperature of overheated surface regions from IR emission spectra, which allows one to determine the temperature of these regions with an accuracy of 10–15 K.

Both X-ray diffraction and IR spectroscopic methods for directly measuring the temperature of nanoparticles of the active component in supported metal catalysts proved the possibility of significant (to 100 K) overheating of these nanoparticles with respect to the inert part of the grain in a catalyst operating in a highly exothermic reaction.

ACKNOWLEDGMENTS

This work was supported by the Ministry of Education of the Russian Federation (grant no. 1-23-00), the state program "Support for Leading Scientific Schools" of Russia (grant no. 00-15-76449), and the grant of the President of the Russian Federation for "Support for Young Russian Scientists and Leading Scientific Schools of Russia" (grant no. NSh-1484.2003.3).

REFERENCES

1. Slin'ko, M.G., Kirillov, V.A., Kulikov, A.V., Kuzin, N.A., and Shigarov, A.B., *Dokl. Akad. Nauk*, 2000, vol. 373, no. 3, p. 359.
2. Slin'ko, M.G., Kirillov, V.A., Mikhailova, I.A., and Fadeev, S.I., *Dokl. Akad. Nauk*, 2001, vol. 376, no. 2, p. 219.
3. Kellow, J. and Wolf, E.E., *Catal. Today*, 1999, vol. 9, p. 47.
4. Parmon, V.N., *Kinet. Katal.*, 1996, vol. 37, p. 476.
5. Gudkov, B.S., Subbotin, A.N., Dykh, Zh.L., and Yakerson, V.I., *Dokl. Akad. Nauk*, 1997, vol. 353, p. 347.
6. Subbotin, A.N., Gudkov, B.S., Dykh, Zh.L., and Yakerson, V.I., *React. Kinet. Catal. Lett.*, 1999, vol. 66, p. 97.
7. Khasin, A.A., Yur'eva, T.M., and Parmon, V.N., *Dokl. Akad. Nauk*, 1999, vol. 367, p. 213.
8. Simonova, L.G., Barelko, V.V., Toktarev, A.V., Paushtis, E.A., Kaichev, V.V., Zaikovskii, V.I., Bukhtiyarov, V.I., and Bal'zhinimaev, B.S., *Kinet. Katal.*, 2001, vol. 42, no. 6, p. 917.
9. Krieger, T.A., Plyasova, L.M., and Yurieva, T.M., *Mater. Sci. Forum*, 2000, vol. 321, p. 386.
10. Tsybulya, S.V., Cherepanova, S.V., and Solov'eva, L.P., *Zh. Strukt. Khim.*, 1996, vol. 37, p. 332.
11. Finkel', V.A., *Vysokotemperaturnaya rentgenografiya metallov* (High-Temperaure X-ray Crystallography for Metals), Moscow: Metallurgiya, 1968.
12. Guinier, A., *Theorie et technigue de la radiocristallographie,* Paris: Dunod, 1956, p. 601.
13. Novikova, S.I., *Teplovoe rasshirenie tverdykh tel* (Thermal Expansion of Solids), Moscow: Nauka, 1974.
14. Plyasova, L.M., Kriger, T.A., Khasin, A.A., and Parmon, V.N., *Dokl. Akad. Nauk*, 2002, vol. 382, no. 4, p. 505.
15. Iveronova, V.I. and Revkevich, G.P., *Teoriya rasseyaniya rentgenovskikh luchei* (Theory of X-ray Scattering), Moscow: Mosk. Gos. Univ., 1972.
16. *Rentgenografiya v fizicheskom metallovedenii* (X-ray Diffraction in Metal Physics), Bagaryatskii, Yu.A., Ed., Moscow: Gosmetallurgizdat, 1961.
17. *Spravochnik khimika* (Chemist's Handbook), Nikol'skii, B.P., Ed., Moscow: Khimiya, 1971, vol. 1.
18. *Rentgenografiya: Spetspraktikum* (X-ray Diffraction: Specialized Practical Course), Katsnel'son, A.A., Ed., Moscow: Mosk. Gos. Univ., 1986, p. 198.
19. Petrov, Yu.I., *Fizika malykh chastits* (Physics of Small Particles), Moscow: Nauka, 1982.
20. Valiev, R.Z. and Aleksandrov, I.V., *Nanostrukturnye materialy, poluchennye intensivnoi plasticheskoi deformatsiei* (Nanomaterials: Preparation by Intensive Plastic Deformation), Moscow: Logos, 2000.
21. Plyasova, L.M., Krieger, T.A., Molina, I.Yu., Ermakova, M.A., and Parmon, V.N., *19th European Crystallographic Meeting*, Nancy, 2000, p. 358.
22. Skryshevskii, A.F., *Strukturnyi analiz zhidkostei i amorfnykh tel* (Structural Analysis of Liquids and Amorphous Solids), Moscow: Vysshaya Shkola, 1980.
23. Blokh, A.G., *Osnovy teploobmena izlucheniem* (Basic Principles of Radiative Heat Transfer), Moscow: Gosenergoizdat, 1962, p. 48.